Pulsed-laser lensing for phase modulation in electron microscopy

Supplementary Information

Daniel X. Du[1,2,3], Adam C. Bartnik[4], Cameron J. R. Duncan[5], Usama Choudhry[6],
Tanya Tabachnik[1], Chaim Sallah[1], Yuki Ogawa[1,2,3], Ebrahim Najafi[7], Ding-Shyue Yang[8],
Jared M. Maxson[4]* & Anthony W. P. Fitzpatrick[1,2,3]*

[1]   Mortimer B. Zuckerman Mind Brain Behavior Institute, Columbia University, New York, NY 10027, USA.

[2]   Department of Biochemistry and Molecular Biophysics, Columbia University, New York, NY 10032, USA.

[3]   Taub Institute for Research on Alzheimer's Disease and the Aging Brain, Columbia University Irving Medical Center, 630 West 168th Street, New York, NY 10032, USA.

[4]   Cornell Laboratory for Accelerator-Based Sciences and Education, Cornell University, Ithaca, New York, NY 14853, USA

[5]   Università degli Studi di Milano-Bicocca, Milan, Italy

[6]   Department of Mechanical Engineering, University of California, Santa Barbara, CA 93106, USA

[7]   The Chemours Company, Wilmington, DE 19899, USA

[8]   Department of Chemistry, University of Houston, Houston, TX 77204, USA

*e-mail: jmm586@cornell.edu; Anthony.Fitzpatrick@columbia.edu

Supplementary Note 1. Simulations

1.1 Derivation

The phase shift (as provided by an integral of the Hamiltonian) is:

$$\phi(\underline{r}) = -\int dt' \frac{1}{\hbar} U(\underline{r}(t'), t')$$

where U is the potential the electron passes through. The interaction potential for the ponderomotive effect is[1]:

$$U(\underline{r}, t) = \frac{e}{2m_e \gamma} \left[A_x^2(\underline{r}(t), t) + A_y^2(\underline{r}(t), t) + \frac{1}{\gamma^2} A_z^2(\underline{r}(t), t) \right] + e\underline{v} \cdot \underline{A}(\underline{r}(t), t) - e\Phi(\underline{r}(t), t)$$

where e and m_e are the constants for the charge and mass of an electron respectively. γ and $\underline{v}$ are the Lorentz factor and the velocity of the electron as dictated by the acceleration voltage. $\underline{A}$ and Φ are the vector and scalar potentials of the laser. We adopt the gauge where the scalar potential is zero and the high frequency photon oscillation negates the dot product term (besides being orthogonal). The vector potential of the laser beam is:

$$\underline{E}(\underline{r}, t) = \epsilon_0 \hat{y} g(y, z) \exp\left[-i\omega_L \left(t - \frac{x}{c} \right) \right] u \left(t - \frac{x}{c} \right)$$

$$\underline{A}(\underline{r}, t) = -\frac{\epsilon_0 \hat{y}}{\omega_L} g(y, z) \sin\left[\omega_L \left(t - \frac{x}{c} \right) \right] u \left(t - \frac{x}{c} \right)$$

with ϵ_0 as the field strength coefficient, c as the speed of light, ω_L as the frequency of the photon, g as the spatial distribution perpendicular to the travel direction, and u as the temporal distribution. Thus, the phase is:

$$
\begin{aligned}
\phi(\underline{r}, t) &\approx -\frac{1}{\hbar} \frac{\epsilon_0^2}{\omega_L^2} \frac{e^2}{2m_e \gamma} \int dt' g^2(x, y, z) u^2 \left(t' - \frac{x}{c} \right) \sin^2\left[\omega_L \left(t' - \frac{x}{c} \right) \right] \\
&= -\frac{1}{\hbar} \frac{\epsilon_0^2}{\omega_L^2} \frac{e^2}{2m_e \gamma} \int dt' g^2(x, y, z) u^2 \left(t' - \frac{x}{c} \right) \left\{ 1 - \cos\left[2\omega_L \left(t' - \frac{x}{c} \right) \right] \right\} \frac{1}{2} \\
&\approx -\frac{1}{\hbar} \frac{\epsilon_0^2}{\omega_L^2} \frac{e^2}{4m_e \gamma} \int dt' g^2(x, y, z) u^2 \left(t' - \frac{x}{c} \right)
\end{aligned}
$$

We can assume the oscillatory sine and cosine terms do not contribute due to the high frequency oscillations of the photons. The laser pulse energy when integrated to infinity is given by:

$$
\begin{aligned}
E_L &= c\varepsilon_0 \epsilon_0^2 \int_{-\infty}^{\infty} dt \, u^2(t) \cos^2(\omega_L t) \int_{-\infty}^{\infty} dydz g^2(y, z) \\
&\approx \frac{c\varepsilon_0}{2} \epsilon_0^2 \int_{-\infty}^{\infty} dt \, u^2(t) \int_{-\infty}^{\infty} dydz g^2(y, z)
\end{aligned}
$$

$$= \frac{c\varepsilon_0}{2} \epsilon_0^2 N_p$$

The shape of the laser pulse is described by a 2D spatial gaussian and a 1D temporal gaussian with the characteristic parameters for laser beam waist ω_0 and laser pulse duration τ_p. The normalization term is thus:

$$g_{00}^2(x,y,z) \propto \exp\left(-\frac{2(y^2+z^2)}{\omega_0^2}\right)$$

$$u^2(x,t) = \exp\left(-\frac{2\left(t-\frac{x}{c}\right)^2}{\tau_p^2}\right)$$

$$N_p = \frac{\omega_0^2 \tau_p}{2}\sqrt{\frac{\pi^3}{2}}$$

Here, we will solely address the magnitude of the phase shift. The phase can be further simplified as:

$$\phi(\underline{r},t) \approx \frac{1}{\hbar}\frac{e^2}{\omega_L^2 m_e \gamma}\frac{E_L}{2c\varepsilon_0}\frac{\int dt' g^2(x,y,z)u^2(x,t')}{N_p} = \frac{1}{\hbar}\frac{e^2}{\omega_L^2 m_e \gamma}\frac{E_L}{2c\varepsilon_0}S(\underline{r},t)$$

$$= \frac{2\pi\alpha E_L}{\omega_L^2 m_e \gamma}S(\underline{r},t) = \frac{\alpha\lambda_L^2 E_L}{\gamma m_e c^2 2\pi}S(\underline{r},t) = \frac{\alpha\lambda_L^2 E_L}{2\pi E_e}S(\underline{r},t)$$

$$S(\underline{r},t)N_p = \int dt' \exp\left[-\frac{2}{\tau_p^2}\left(t'-\frac{x}{c}\right)^2\right]\exp\left[-\frac{2}{\omega_0^2}(z^2+y^2)\right]$$

By considering the positions (x,y,z) as functions of time for a traveling electron, the phase shift is:

$$\phi(\underline{r},t) \approx \frac{\alpha\lambda_L^2 E_L}{2\pi E_e}\frac{1}{N_p}\int dt' \exp\left[-\frac{2}{\tau_p^2}\left(t'-\frac{x}{c}\right)^2\right]\exp\left[-\frac{2}{\omega_0^2}(z^2+y^2)\right]$$

Phase is inherently difficult to measure. Instead, we measure the deflection caused by passing the electron through the laser beam. We expect the laser to roughly behave as a concave lens that is stronger in the axis perpendicular to the direction of laser travel. The momentum shifts are thus:

$$\delta\underline{p} = \hbar\nabla\phi(\underline{r},t)$$

$$\underline{\nabla}\phi(\underline{r},t) = \frac{\hbar\alpha\lambda_L^2 E_L}{2\pi E_e}\frac{\nabla\int dt' g^2(x,y,z(t'))u^2\left(t'-\frac{x}{c}\right)}{N_p}$$

$$= \frac{\hbar\alpha\lambda_L^2 E_L}{2\pi E_e N_p}\int dt'\underline{\nabla}\left[g^2(x,y,z)u^2\left(t'-\frac{x}{c}\right)\right]$$

$$\Delta p_x = \frac{\hbar \alpha \lambda_L^2 E_L}{2\pi E_e N_p} \int dt' \left\{ \frac{4\left(t - \frac{x}{c}\right)}{c\tau_p^2} \exp\left[-\frac{2\left(t - \frac{x}{c}\right)^2}{\tau_p^2} - \frac{2(y^2 + z^2)}{\omega_0^2} \right] \right\}$$

$$\Delta p_y = \frac{\hbar \alpha \lambda_L^2 E_L}{2\pi E_e N_p} \int dt' \left\{ -\frac{4y}{\omega_0^2} \exp\left[-\frac{2\left(t' - \frac{x}{c}\right)^2}{\tau_p^2} - \frac{2(y^2 + z^2)}{\omega^2(x)} \right] \right\}$$

1.2 Assumptions

Application of the equations above make the following assumptions of the experiment:

1. The laser and electron beams interact in such a small region relative to the travel distance of the electron beam that the momentum and phase shifts are instantaneously applied to the travel path of the electron beam. We have found this to be accurate in cases where the laser and electron pulse durations are at least shorter than 1 ns [2].

2. The gaussian beam profile has a best-fit to the fundamental transverse-electromagnetic (TEM$_{00}$) solution to the laser gaussian beam and ignores any fringes that may appear due to dust, mirror, or lens aberrations.

3. The photon oscillatory component (582 THz, ~1.7 fs period) truly plays no part on the timescales involved in the ponderomotive interaction (140 fs for the electrons to cross the interaction zone).

4. The effect can be averaged across varying electron pulse durations (due to fluctuations in electron counts) to be equivalent to an experiment performed at the average pulse duration.

1.3 Parameters used in simulations

In Figure 1 of the main text, we show a simulation that provides a reasonable match to the data collected by experiment. The properties of the electron beam and laser beam used in that simulation are described in the table below.

Table S1. Experimental parameters

Parameter	Used Value	Value Range
Magnification	15kx	10kx-20kx
Interaction to Sample	7000 μm	7000 μm[a]
Focus to Sample	-200 μm	0 to -630 μm[b]
Interaction Size	15 μm	12 to 24 μm[c]
Laser Bunch (s.d.)	212 fs	>212 fs[d]
Electron Bunch	6200 fs	5200 to 7200 fs[e]
Laser Focus	12.5 μm	12.4 to 12.6 μm[f]
Electron Focus	1 nm	>1nm[g]
Electron Rotation	-70º	-30º to -90º [h]
Electron Astigmatism ($\perp$/‖)	0.5	0.25 to 0.75[h]
Electron Energy	30 keV	30 keV
Laser Pulse Energy	3.21 μJ/pulse	3.21 μJ/pulse[i]
Laser Wavelength	515 nm	515 nm[d]
Laser Positional Offset ($\perp$)	1.75 μm	1.75 μm[e]

[a]This is set by the position of the specimen stage
[b]This is the defocus range that the electron beam shifts by when moving from thermionic/Schottky mode to photoelectron mode
[c]As shown in Figure S2.
[d]Property of the laser, 500 fs fwhm
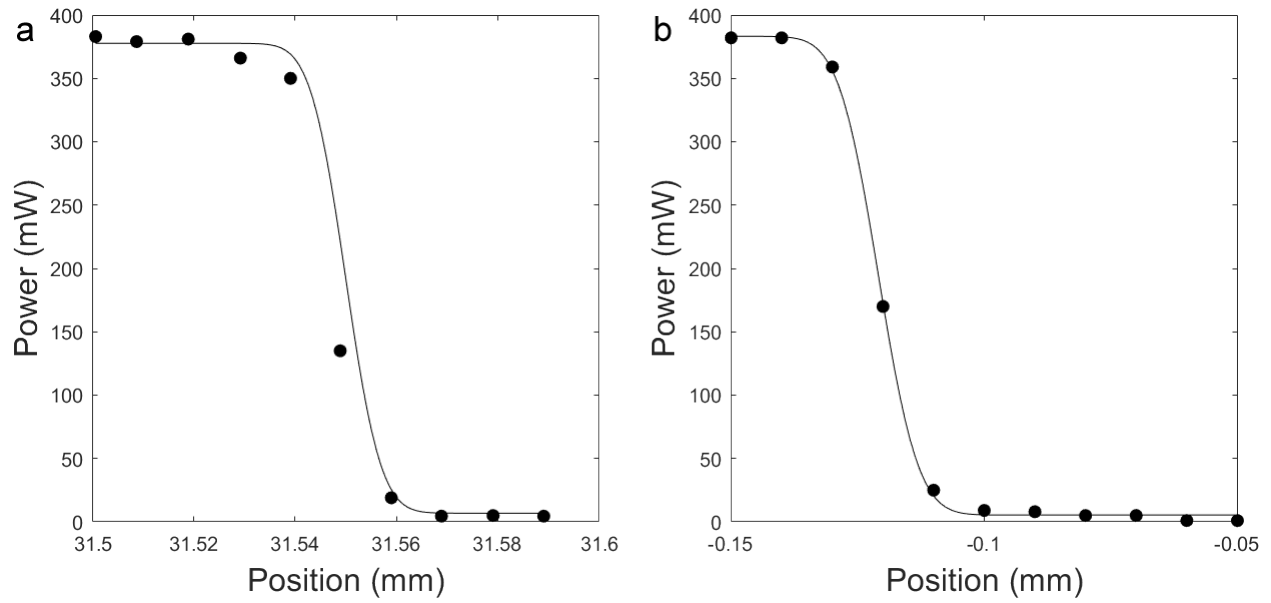[e]As shown in Figure 2a of the main text
[f]As shown in Figure S1.
[g]Theoretical resolution limit of the SEM.
[h]As shown in Figure S2.
[i]Measured at a known position in the laser line

Laser Parameters

Figure S1. Size of the pump laser beam in the two directions perpendicular to the Poynting vector. Beam sizes are determined with a silicon knife edge within the microscope. **a,** The plot for the direction parallel to the electron beam. The size measured here is 12.6 microns. **b,** The plot for the direction perpendicular to both the Poynting vector of the laser and the electron beam. The size from the fit is 12.4 microns.

Electron Beam Parameters
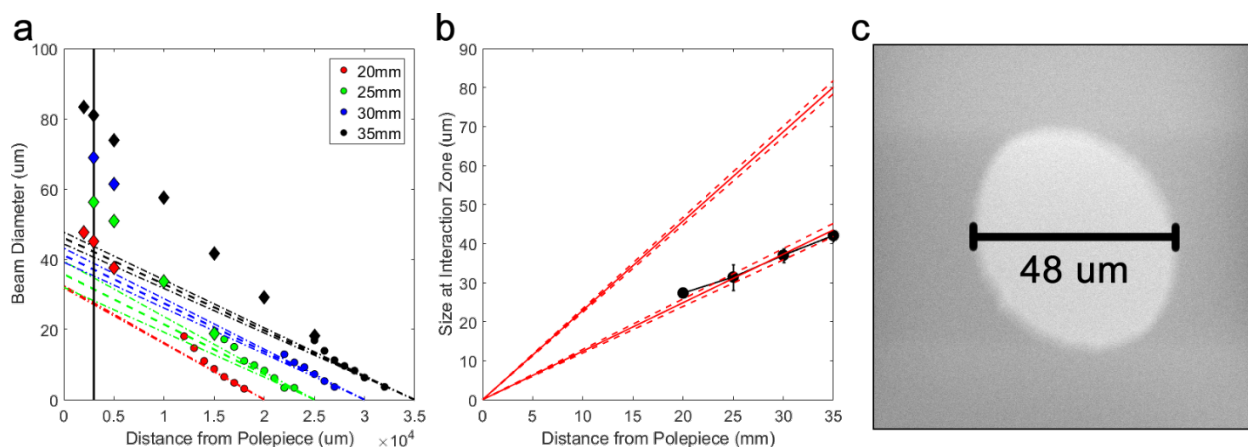
Figure S2. Size of the electron beam at various distances from the focal point. a, The electron beam ideally linearly increases in size as it moves further away from the working distance (focal point). The working distance is set to a specific position (indicated by color) and measurements of the beam size are acquired by imaging a small piece of dust and dividing the resulting size dimensions by a factor of two. These dimensions are plotted as a function of distance from the polepiece. **b,** When the 1000 micron aperture is used, the size of the electron beam in the interaction region (7 mm) is 12 to 24 microns. These two values are derived from the information found by the non-linear data (**a**) split into a far-field set and a near-field set. The true beam size must be intermediate in value. This value is used in the simulations (see Supplementary Note 1 and Supplementary Table S1). **c,** A description of the electron beam size 3mm from the polepiece. The true size of the electron beam must be divided by a factor of two.

Control experiment

To ensure the effect we observed was central to the interaction region between the laser and the electron beam, we performed an additional control. The specimen was moved 23.5 mm away from the interaction zone. If the observed effect was dependent on the surface of the specimen, then the time-zero position[3,4] would move. Here, we observed no difference in time-zero, ensuring that the effect we observed is localized to the laser-electron interaction zone.
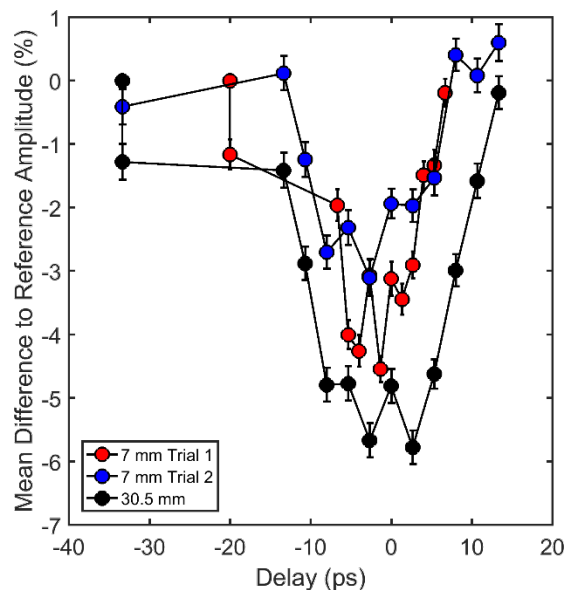
Figure S3. Interaction control to ensure no surface effect. The same trials from the 0.5 nJ/pulse experiments from Figure 2 of the main text are repeated here, including the reference images. A third experiment involving the moved specimen set to 30.5 mm away from the polepiece is also overlayed on the image. We can see that t_0 has not moved by an expected 23.5 mm on the delay stage (more than 100 ps).

References

1. Mihaila, M. C. C., *et al.* Transverse Electron Beam Shaping with Light. *Phys. Rev. X* **12**, 031043 (2022).
2. Du, D. X. & Fitzpatrick, A. W. P. Design of an ultrafast pulsed ponderomotive phase plate for cryo-electron tomography. *Cell Reports Methods* **3**, 100387 (2023).
3. Yang, D.-S., Mohammed, O. F. & Zewail, A. H. Scanning ultrafast electron microscopy. *Proc. Natl. Acad. Sci.* **107**, 14993-14998 (2010).
4. Du, D. X., *et al.* Development of an ultrafast pulsed ponderomotive phase plate for cryo-electron tomography. *bioRxiv* 2024.03.20.585981 (2024).